To the problem of atmospheric correction of satellite data in space monitoring of small-sized forest fire sources

S.V. Afonin

Institute of Atmospheric Optics,
Siberian Branch of the Russian Academy of Sciences, Tomsk

The reconstruction of brightness characteristics of two small-sized stationary high-temperature objects (located at the territory of Tomsk Region) based on NOAA measurements and the use of routine information on actual optical-meteorological and geometrical conditions of satellite observations is described.

Introduction

The remote sensing of underlying surface from space favors solving the topical problem of prompt detection of forest and industrial fires. It is important to detect a fire at early stage of its development (area of less than 5−10 hectares) when the fire extinction does not require serious efforts. At present, in the global monitoring of forest fires the NOAA/AVHRR instruments with spectral channels $\lambda = 0.63$ μm (No. 1), 0.84 μm (No. 2), 1.6 μm (No. 3a), 3.75 μm (No. 3), 10.8 μm (No. 4), and 12.0 μm (No. 5) are widely used, as well as the EOS/MODIS instrument (36 spectral channels) having a maximal space resolution (MSR) about 1 km^2. In this case, it is necessary to have reliable algorithms for automated recognition of small-sized high-temperature anomalies with an area less than 0.1% of MSR on the satellite infrared images. To obtain the maximal accuracy, it is profitable to conduct the atmospheric correction of satellite infrared measurements using the information about meteorological and aerosol characteristics of the atmosphere and accounting for the geometry of observations.

Analysis of available data on the algorithms for detection of fire sources from space[1–3] enabled us to draw the following conclusion. Most usable algorithms apply the deciding rule $P\{x\} > \mathrm{d}P,$ where $\mathrm{d}P$ is the threshold value of the function $P\{x\}$, and its parameters $\{x\}$ are commonly the airspace measurements of albedo and brightness temperatures (or their functions). The $\mathrm{d}P$ is fixed or can be determined based on statistical characteristics calculated for $\{x\}$ in the vicinity of a potential fire. The simplest version uses as $\{x\}$ the brightness temperature T_3 of the third channel ($\lambda = 3.75$ μm) and the difference in temperatures $\mathrm{d}T_{34}$ in channels No. 3 and No. 4. However, the usable algorithms do not actually take into account in the explicit form the optical-geometric conditions of the satellite measurements.

At the Institute of Atmospheric Optics SB RAS, the investigations of distorting atmospheric effect on the results of satellite monitoring of underlying surface are performed.[4–9] In this paper, an attempt is made to determine the brightness characteristics of two small-sized stationary high-temperature objects, located in the Tomsk Region, based on the NOAA satellite measurements and the use of routine information on actual optical-meteorological and geometric conditions of the satellite observations.

1. Spaceborne retrieval of brightness characteristics of a small-sized fire source

Let us present basic relationships[9] for the algorithm of spaceborne retrieving of brightness characteristics of small-sized fires.

Let at a certain part of underlying surface (US) of the area S_0, corresponding to the angle of the radiometer field of view, and the temperature T_0 be a small-sized fire of the area S_f ($S_f \ll S_0$) and the temperature T_f ($T_f = 600-1200$ K).

The intensity I_λ of the upgoing flux of thermal radiation can be written as follows:

$$I_\lambda = B_\lambda(T_\lambda), \quad I_\lambda = I_{\mathrm{hot}} + I_{\mathrm{bg}}, \tag{1}$$

where $B(T_\lambda)$ is the Planck function, T_λ is the radiation temperature of thermal radiation; I_{hot} is the intensity of the fire centre attenuated by the atmosphere, I_{bg} is the background radiation intensity.

The contribution of thermal radiation to the measured intensity I_λ can be written in the form:

$$I_{\mathrm{hot}} = B_{\mathrm{hot}}P_\lambda, \quad B_{\mathrm{hot}} = R(\theta)\varepsilon_\lambda^{\mathrm{f}}B_\lambda(T_f), \quad R(\theta) = S_f/S_0(\theta),$$

where $P_\lambda = \exp\{-\tau_\lambda/\cos(\theta)\}$ is the atmospheric transmittance; τ_λ is the atmospheric optical depth; θ is the scanning angle of the instrument axis; $\varepsilon_\lambda^{\mathrm{f}} \approx 1$ is the emittance of the thermal source.

The background contribution to the measured intensity I_λ can be presented as a sum of four components:

$$I_{\mathrm{bg}} = I_{\mathrm{srf}} + I_{\mathrm{atm}} + I_{\mathrm{rfl}} + I_{\mathrm{sct}}, \tag{2}$$

where I_{srf} is the contribution of the surface thermal radiation attenuated by the atmosphere; I_{atm} is the

contribution of the atmospheric thermal radiation, I_{rfl} is the contribution of solar radiation fluxes incident and reflected from the surface, and I_{sct} is the contribution of heat and solar radiation fluxes scattered by the atmosphere.

Note that

$$I_{srf} = [1 - R(\theta)]\,\varepsilon_\lambda^0 B_\lambda(T_0) P_\lambda, \qquad (3)$$

where ε_λ^0 is the emittance of the underlying surface; T_0 is the background temperature of the underlying surface;

$$I_{atm} = f\{\theta,\, T(h),\, \tau_\lambda(h)\} \qquad (4)$$

depends on vertical profiles of temperature and characteristics of atmospheric extinction.

$$I_{rfl} = A_\lambda P_\lambda f_\lambda^{rfl}(Z,\, met,\, ext,\, sct), \qquad (5)$$

where A_λ is the underlying surface albedo;

$$I_{sct} = f_\lambda^{sct}(\theta,\, \varphi,\, Z,\, met,\, ext,\, sct). \qquad (6)$$

The following designations are used in Eqs. (2)–(6):

— geometric parameters of observations ($\theta,\, \varphi,\, Z$): the slope angle of the instrument axis, solar zenith angle, the relative azimuth of measurements;

— atmospheric characteristics: meteorological (met), heat radiation extinction (ext), and heat radiation scattering (sct).

From the viewpoint of correct consideration of optical-geometric conditions of observations, the problem of detection from space of a small-sized high-temperature object should be solved by reconstructing in the third channel AVHRR ($\lambda = 3.75\ \mu m$) of the radiation intensity B_{hot} of a small-sized thermal source

$$B_{hot} = (I_3 - I_{bg})/P_3, \qquad (7)$$

where I_3 is the measured intensity of heat radiation, and the values of I_{bg} and P_3 are calculated based on *a priori* optical-meteorological information.

In this case, the deciding rule of detection of the forest fire source $B_{hot} > dB$ from space will be independent of optical-geometric conditions of observation. To attain this aim, the information on characteristics of underlying surface and optical and meteorological atmospheric parameters is necessary.

2. An example of atmospheric correction of satellite data in the problem of detection of small-sized high-temperature objects from space

The considered in Section 1 approach to the atmospheric correction of results of satellite monitoring of high-temperature objects (HTO) was used in the processing of NOAA/AVHRR satellite data. Figure 1 shows a fragment of the image obtained in the morning (at 07:56 LT) May 21, 2001 from the NOAA-14 satellite.
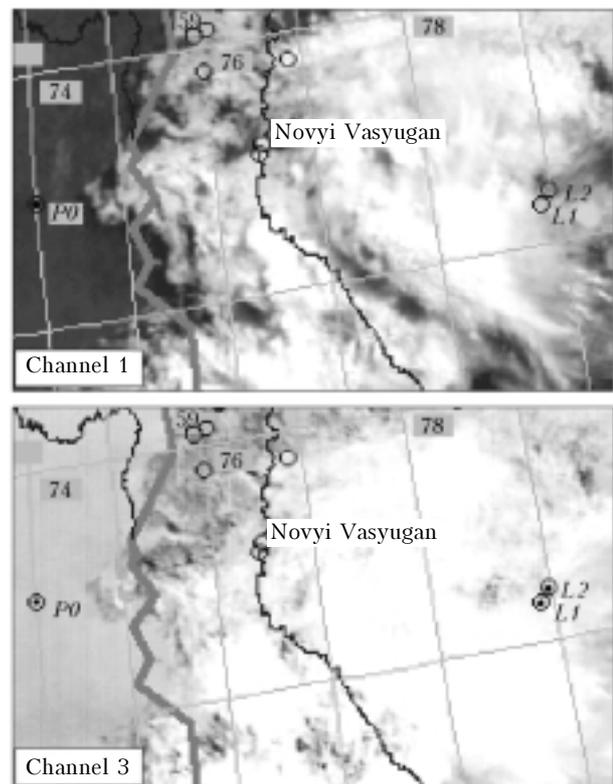

Fig. 1. A fragment of the space image of two high-temperature objects *L1* and *L2*; the point *P0* is characterized by cloudless conditions; NOAA-14 satellite data: May 21, 2001; local time: 07:56; Spectral channels AVHRR: 0.63 μm (No. 1) and 3.75 μm (No. 3).

In the fragment (channel 3), two stationary high-temperature objects (points *L1* and *L2*) are well observed. The observation of these HTOs from space is characterized by rather poor optical conditions, due to inhomogeneous semitransparent cloudiness in the vicinity of *L1* and *L2*. By the visual data, a higher optical density of cloudiness should be noted just around the point *L1*.

In the image, the point *P0* is marked characterized by cloudless conditions during satellite measurements. The data obtained in the vicinity of this point enable us to estimate the meteorological parameters of the atmosphere (vertical profiles of temperature and humidity) and the background temperature of the underlying surface.

The characteristics measured at *L1*, *L2*, and *P0* (albedo A_1, A_2 and brightness temperatures T_3, T_4, T_5) are presented in Table 1.

Analysis of data from Table 1 together with data from Refs. 1–3 has made it possible to conclude that the successful detection of the object *L2* due to high brightness temperature ($T_3 = 322$ K) will not be a particular problem for most usable algorithms of detecting forest fires. At the same time, the automated detection of the object *L1* cannot be realized because of a relatively low value of T_3 (293 K) and a relatively high value of albedo A_1 (8.38%) in the channel 1 of AVHRR.

Table 1. Characteristics of measurements with AVHRR/NOAA instrument at the points *L1*, *L2*, and *P0*

Points	Characteristics of measurements				
	A_1, %	A_2, %	T_3, K	T_4, K	T_5, K
L1	**8.38**	**8.80**	**293.03**	**259.25**	**256.89**
	8.59	8.79	273.72	260.06	258.19
	1.35	1.20	4.51	3.27	3.16
L2	**5.77**	**6.40**	**322.61**	**268.42**	**266.16**
	5.78	6.09	276.91	266.80	264.84
	1.06	1.11	8.03	2.61	2.50
P0	**3.02**	**3.84**	**281.34**	**280.00**	**278.98**
	2.98	3.73	280.22	279.86	278.93
	0.11	0.09	0.46	0.15	0.14

N o t e . For every point, the second line is the mean value (for the "window" 9×9 pixels) and the third line is its root-mean-square deviation.

The thematic processing of the fragment of the space image (Fig. 1) was performed as follows.

1. To define the parameters of the atmospheric meteorological conditions, the vertical profiles of temperature and humidity closest to the point *P0* were used, obtained based on measurements of an atmospheric TOVS/NOAA sounder.

2. The background temperature of the underlying surface (TUS) T_0 was assessed using the single-channel [taking into account Eq. (2)] and double-channel techniques[11] at the point *P0* based on the infrared measurements of the fourth and fifth AVHRR channels using the meteorological TOVS/NOAA data. As a result, $T_0 \approx 283$ K was obtained.

3. Using AVHRR measurements and models of atmospheric aerosol and cloudiness[12] in combination with the methods described in Refs. 9 and 10, the atmospheric optical parameters were determined.

4. The values of B_{hot} (see Eq. (7)) were determined at points *L1* and *L2* (Table 2), as well as parameters I_{bg} and P_3 required for retrieving the brightness characteristics of high-temperature objects were estimated.

Table 2. Results of retrieval of heat radiation intensity of high-temperature objects

Points	I_3, $\dfrac{\text{mW}}{\text{m}^2 \cdot \text{sr} \cdot \text{cm}^{-1}}$	τ_3^{aer}	P_3	I_{bg}, $\dfrac{\text{mW}}{\text{m}^2 \cdot \text{sr} \cdot \text{cm}^{-1}}$	B_{hot}, $\dfrac{\text{mW}}{\text{m}^2 \cdot \text{sr} \cdot \text{cm}^{-1}}$
L1	0.5032	2.64	0.0545	0.2602	4.4587 (355.5 K)
L2	1.6500	1.11	0.2511	0.2965	5.3903 (358.8 K)

The retrieved values of B_{hot} are equivalent to the values of the radiation temperature exceeding 355 K (82°C) that enables us to confirm with confidence the presence of high-temperature objects both at *L2* and at *L1.*

Conclusion

Thus, despite the poor optical-geometric conditions of observations, the problem of automatic detection of high-temperature objects of type *L1* can be solved due to performing the atmospheric correction, if:

– to assess the initial information (optical-meteorological atmospheric parameters, values of background temperature of underlying surface) based on the ground-based and space data, actual for the time of conducting space measurements;

– to calculate the required characteristics (1)–(6) by the numerical simulation methods and based on initial optical-meteorological information;

– to determine by Eq. (7) the intensity of a high-temperature object.

Acknowledgments

References

1. V.V. Belov, ed., *Satellite Monitoring of Forest Fires in Russia. Results, Problems, Perspectives* (Novosibirsk, SB RAS IAO, GPNTB, 2003), 135 pp.
2. Y.J. Kaufman and C.O. Justice, MODIS ATBD Fire Products, (Version 2.2, Nov. 10, 1998), EOS, ID#2741 (1998), 77 pp.
3. S.H. Boles and D.L. Verbyla, Remote Sensing of Environ. **72**, 1–16 (2000).
4. S.V. Afonin, *"Development and application of the atmospheric radiation model for determining the temperature of ocean surface on the basis of satellite sensing data,"* Cand. Phys.-Math. Sci. Dissert., Tomsk (1987), 192 p.
5. S.V. Afonin, V.V. Belov, and I.Yu. Makushkina, Atmos. Oceanic Opt. **10**, No. 2, 114–118 (1997).
6. V.V. Belov, S.V. Afonin, Yu.V. Gridnev, and K.T. Protasov, Atmos. Oceanic Opt. **12**, No. 10, 951–956 (1999).
7. V.V. Belov and S.V. Afonin, Proc. SPIE **4725**, 471–478 (2002).
8. V.V. Belov and S.V. Afonin, in: *Abstracts of Reports at International Symposium of SIC countries on Atmospheric Radiation "MCAP-2",* St.-Petersburg (2002), pp. 96–97.
9. S.V. Afonin and V.V. Belov, Computational Technologies **8**, Special issue, 35–46 (2003).
10. S.V. Afonin, V.V. Belov, B.D. Belan, M.V. Panchenko, S.M. Sakerin, and D.M. Kabanov, Atmos. Oceanic Opt. **15**, No. 12, 1015–1019 (2002).
11. J.C. Price, J. Geophys. Res. **89**, 7231–7237 (1984).
12. F.X. Kneizys, E.P. Shettle, G.P. Anderson, L.W. Abreu, J.H. Chetwynd, J.E.A. Selby, S.A. Clough, and W.O. Gallery, *User Guide to LOWTRAN-7,* AFGL-TR-86-0177, ERP No. 1010, Hanscom AFB, MA 01731.